Electronic supplenmentary information for

Efficient photoelectrocatalytic performances with $WO_3/BiVO_4$ heterojunction photoanode: applied bias-promoted photoinduced charge transfer and separation

Yunni Liu,[a] Yuna Kang,[a] Zhenyi Zhang[b] and Jun Lin*[a]

[a] School of Chemistry and Life Resources, Renmin University of China, Beijing 100872, P. R. China.

*Email: jlin@ruc.edu.cn

[b] Key Laboratory of New Energy and Rare Earth Resource Utilization of State Ethnic Affairs Commission, Key Laboratory of Photosensitive Materials & Devices of Liaoning Province, School of Physics and Materials Engineering, Dalian Minzu University, Dalian 116600, P. R. China.

1. Calculation of the applied bias photon to current efficiency (ABPE) [1, 2]

The applied bias photon to current efficiency (ABPE) is calculated from the LSV curve to assess the PEC performance of different photoanodes using the following equation:

$$\mathrm{ABPE} = \frac{J_{ph}\,(1.23 - V)}{P_{light}} \qquad (1)$$

where J_{ph} represents the photocurrent density, V is the applied bias, P_{light} is the power density of the incident light.

2. Calculation of charge separation and charge injection efficiencies [3-6]

The photocurrent density generated by PEC water oxidation can be described by the following formula:

$$J_{PEC} = J_{absorbed} \times P_{charge\ separation} \times P_{charge\ injection} \qquad (2)$$

where $J_{absorbed}$ represents the photocurrent density generated by the complete conversion of the absorbed irradiation absorbed by the material, which is constant with fixed semiconductor photocatalyst and lighting source. $J_{absorbed}$ can be calculated using the following equation:

$$J_{absorbed} = J_{max} \times \mathrm{LHE} \qquad (3)$$

where LHE is light-harvesting efficiency ($\mathrm{LHE} = 1 - 10^{-A_{(\lambda)}}$, $A_{(\lambda)}$ is the absorbance at specific wavelength λ), and J_{max} is the maximum photocurrent density achievable assuming 100% IPCE for photons with higher

energy than the bandgap of the photoanode. This was performed by the conversion of a 300 W xenon lamp (LabSolar II, Perfect Light Co., Ltd) equipped with a UV-cutoff filter ($\lambda \geq 420$ nm) from radiation energy (W m^{-2} nm^{-1}) to number of photons (s^{-1} cm^{-2} nm^{-1}) using the Equation (4) for each wavelength:

$$\text{number of photons} = \left(\frac{\text{radiation energy}}{\left(\frac{c \times h}{\lambda} \right)} \right) \times \frac{1\ m^2}{10000\ cm^2} \qquad (4)$$

where radiation energy is the energy for each wavelength in the reference spectrum (unity in W m^{-2} nm^{-1}). c is 2.99×10^8 m s^{-1} (speed of light in a vacuum). h is 6.63×10^{-34} J s (Planck constant) and λ is the wavelength of photon (unity in m).

Next, the number of photons is converted to mol of photons using the Equation (5):

$$\text{mol of photons} = \text{number of photons} / N_A \qquad (5)$$

where N_A is 6.022×10^{23} (Avogadro constant). Then, the mol of photons is converted to current (mA) using the Equation (6):

$$\text{current (mA)} = (\text{mol of photons}) \times F \times 1000 \qquad (6)$$

in which F is 96485.33 C mol^{-1} and 1000 is a constant to result the unity at mA cm^{-2} nm^{-1}.

In this way, the theoretical maximum photocurrent density J_{max} was determined by trapezoidal integration of the photocurrent spectrum (mA cm^{-2} nm^{-1}) as a function of wavelength (nm) above the optical bandgap of the photoanodes. The bandgaps of WO_3 and $WO_3/BiVO_4$-15 were determined by diffuse reflectance spectroscopy (DRS) to be 2.70 eV and 2.55 eV, respectively. Base on the experimental data (**Fig. S9**), the $J_{absorbed}$ was calculated to be 7.55 mA cm^{-2} for WO_3 and 10.02 mA cm^{-2} for $WO_3/BiVO_4$-15.

Moreover, $P_{charge\ separation}$ is the charge separation yield of the photogenerated charge carriers. $P_{charge\ injection}$ is the charge injection yield from electrode to electrolyte, reflecting the efficiency of water oxidation process. This equation describes energy losses occurring at different stages of the PEC water oxidation reaction. To evaluate the efficiency of each process, the widely used hole scavenger Na_2SO_3 (0.1 M) was added to the electrolyte (0.5 M Na_2SO_4) to completely consume the holes accumulated on the surface. By this way, the charge injection efficiency was assumed to be 100%, allowing for the precise determination of charge separation efficiency. As described above:

$$J_{Na_2SO_3} = J_{absorbed} \times P_{charge\ separation} \qquad (7)$$

Therefore, the charge separation efficiency can be calculated as follows:

$$P_{charge\ separation} = J_{Na_2SO_3} / J_{absorbed} \quad (8)$$

$$P_{charge\ injection} = J_{PEC} / J_{Na_2SO_3} \quad (9)$$

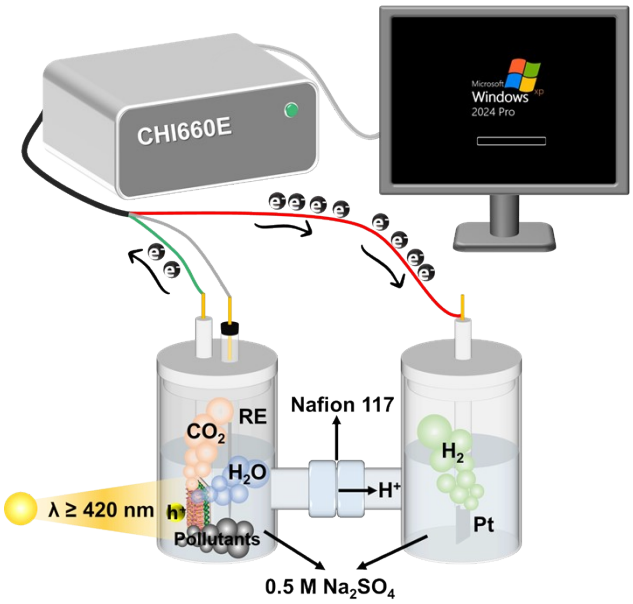

Fig. S1 Schematic illustration for PEC system using the WO_3/$BiVO_4$-15 photoanode.

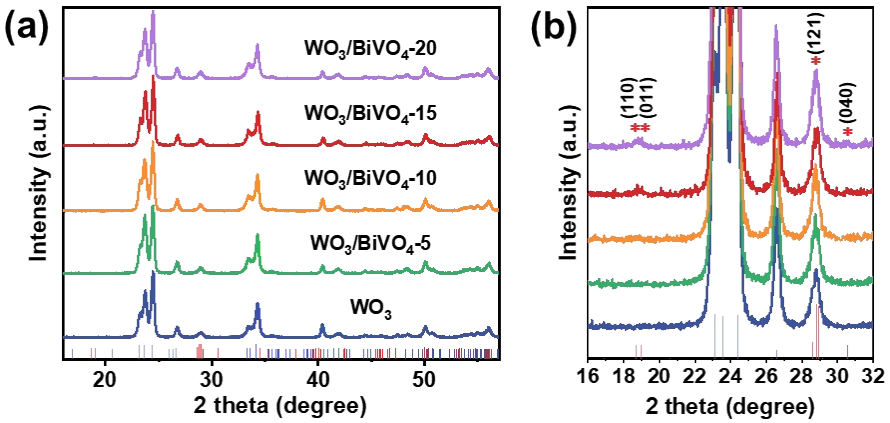

Fig. S2 (a) Wide-angle XRD patterns and (b) magnified XRD patterns in the range of 16−32°.

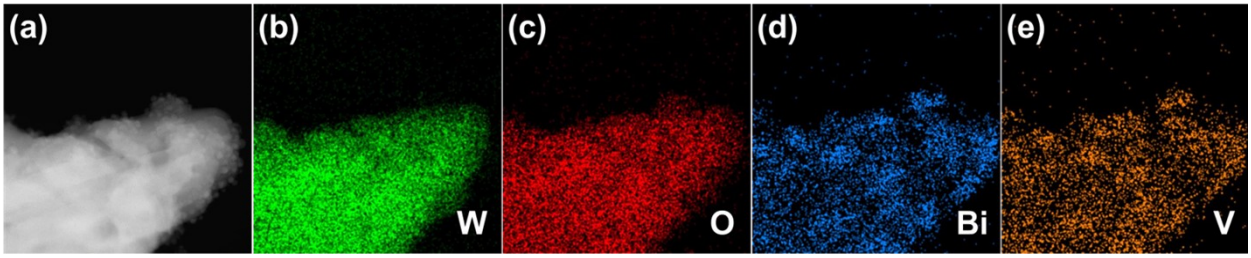

Fig. S3 (a) TEM image of WO_3/$BiVO_4$-15 for TEM-EDS mapping and the corresponding EDS element maps of

(b) W, (c) O, (d) Bi, (e) V, respectively.

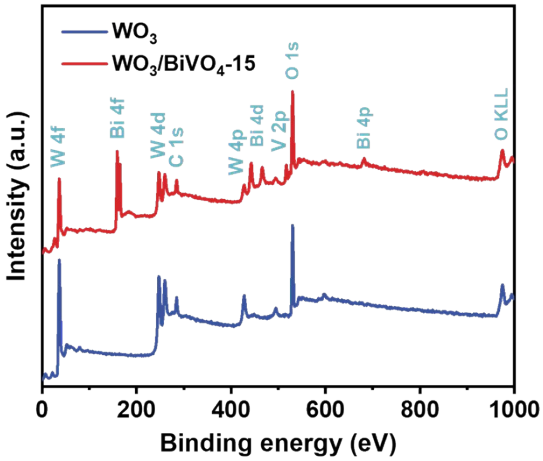

Fig. S4 XPS survey spectra of WO_3 and $WO_3/BiVO_4$-15.

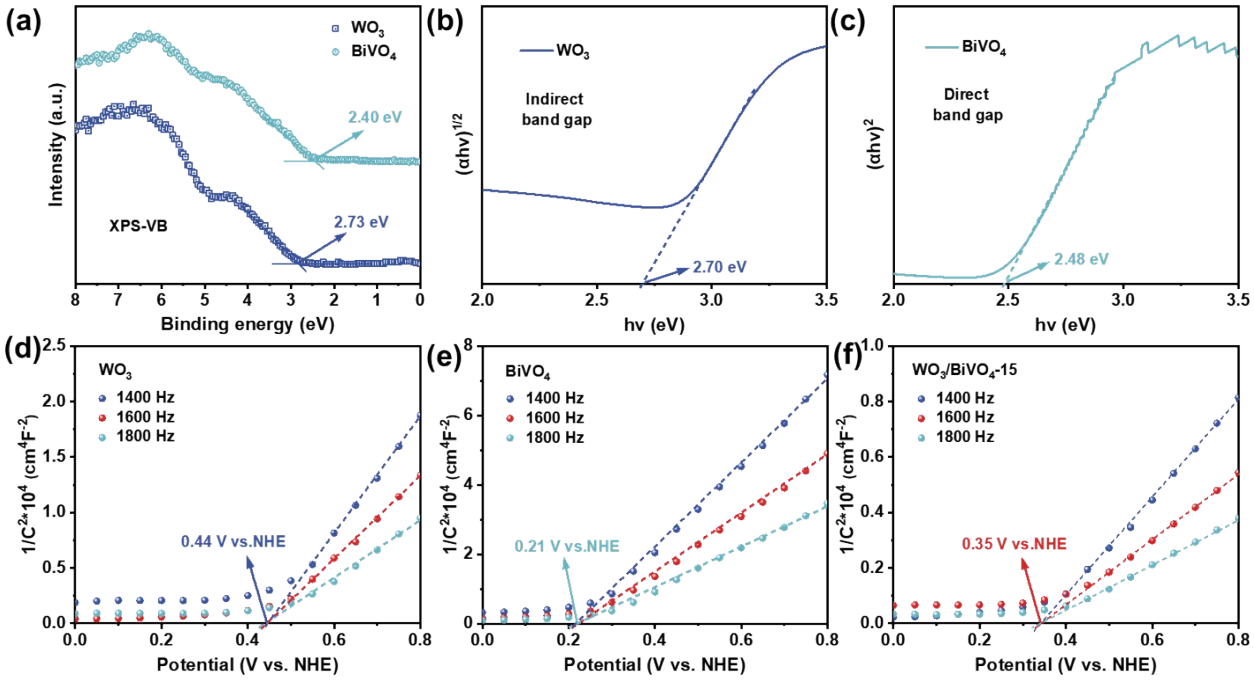

Fig. S5 (a) XPS-VB spectra. (b-c) Tauc plots of WO_3 and $BiVO_4$. (d-f) Mott−Schottky plots of WO_3, $BiVO_4$ and $WO_3/BiVO_4$-15 photoanodes measured at fixed frequencies of 1400, 1600 and 1800 Hz.

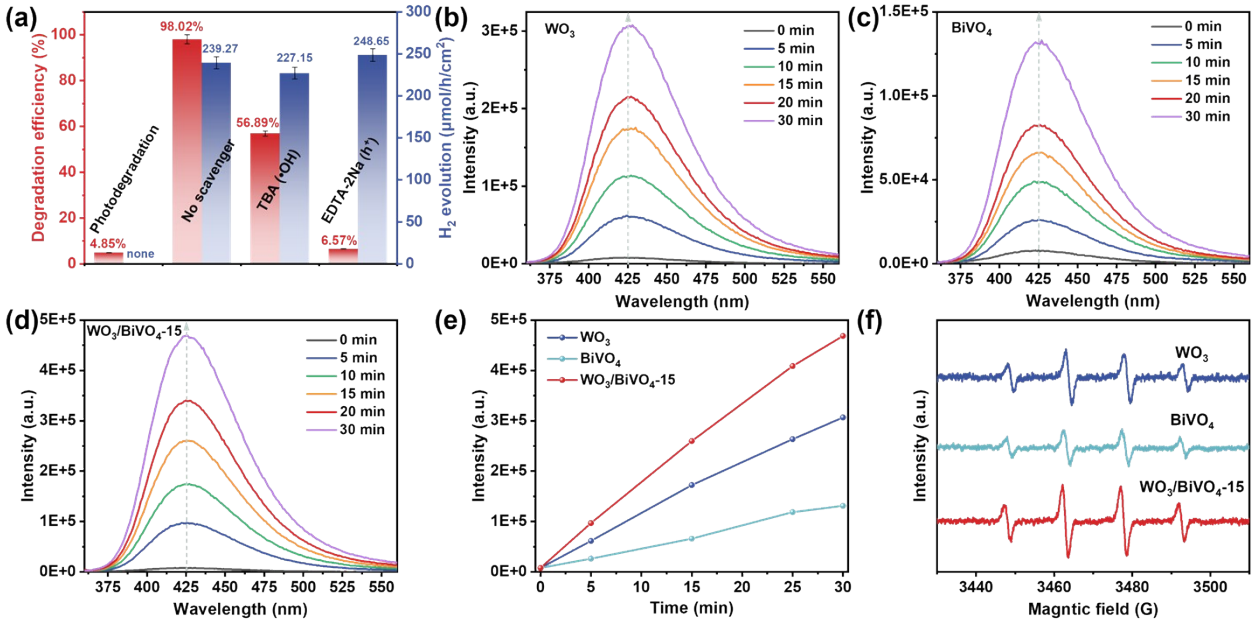

Fig. S6 (a) PEC performances for RhB degradation coupled with simultaneous cathodic H_2 evolution using the $WO_3/BiVO_4$-15 photoanode in the presence of different scavengers. (b-e) PL spectra of the reaction solution for WO_3, $BiVO_4$ and $WO_3/BiVO_4$-15 photoanodes with increasing PEC reaction time (excitation at 315 nm). (f) ESR spectra obtained with DMPO as a trapping agent after 1 h reaction for WO_3, $BiVO_4$ and $WO_3/BiVO_4$-15 photoanodes in PEC process.

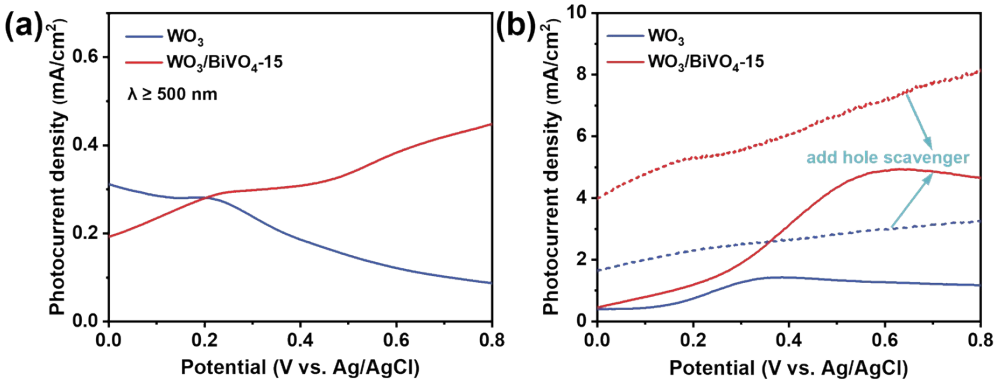

Fig. S7. (a) LSV curves of WO_3 and $WO_3/BiVO_4$-15 photoanodes measured in 0.5 M Na_2SO_4 electrolyte under visible-light irradiation (λ≥500 nm). (b) LSV curves measured in 0.5 M Na_2SO_4 electrolyte under visible-light irradiation (λ≥420 nm) with and without a hole scavenger.

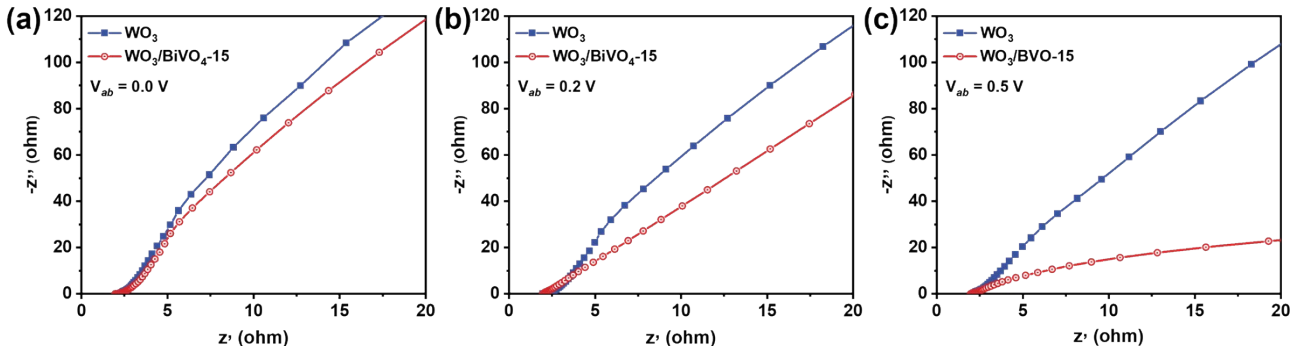

Fig. S8 (a), (b), and (c) EIS spectra of WO_3 and $WO_3/BiVO_4$-15 photoanodes under different applied bias potentials.

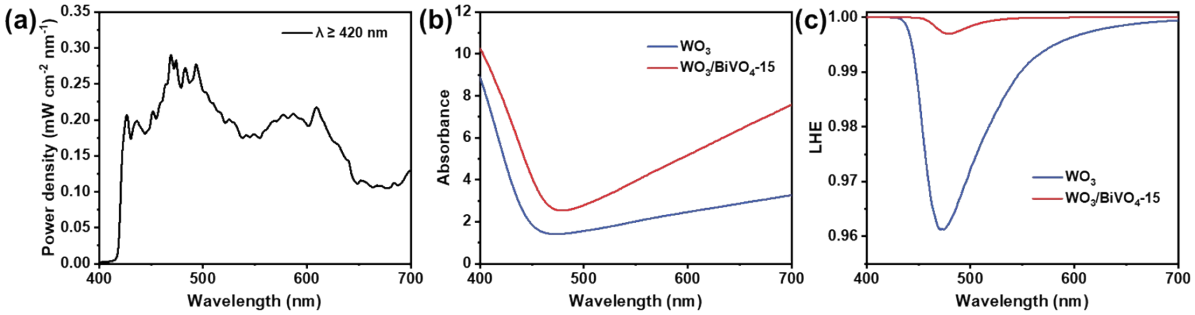

Fig. S9 (a) Visible-light irradiation spectrum of a 300 W xenon lamp equipped with a UV-cutoff filter ($\lambda \geq 420$ nm) showing the power density (mW cm^{-2} nm^{-1}) as a function of wavelength. (b-c) UV-vis absorption spectra and light harvesting efficiencies of WO_3 and $WO_3/BiVO_4$-15 photoanodes.

Table S1. Comparison of our work with the recent WO_3 heterojunction photoanodes in PEC system.

Photoanode	Electrolyte	Photocurrent	H_2 and O_2 evolution/ Pollutants removal	References
Surface dispersed $BiVO_4/WO_3$ nanoplates	0.2 M KPi buffer Solution	3.53 mA/cm^2 at 1.23 V *vs.* RHE	H_2: - O_2: -	7
$WO_3/BiVO_4$/OER (FeOOH/NiOOH)	0.5 M Na_2SO_3	5.0 mA/cm^2 at 1.23 V *vs.* RHE	H_2: 145 µmol/cm^2 O_2: 70 µmol/cm^2 (120 min)	8
F:FeOOH/$BiVO_4/WO_3$	0.1 M KPi buffer solution	3.1 mA/cm^2 at 1.23 V *vs.* RHE	H_2: - O_2: -	9
WO_3 with hexagonal-monoclinic heterophase junction supported on W mesh (hm-m-WO_3/W mesh)	0.1 M Na_2SO_4	5.6 mA/cm^2 at 1.2 V *vs.* RHE	99.9% of 20 ppm BPA; 60.9% of TOC (150 min)	10

$CoOOH/WO_3$	0.1 M Na_2SO_4	3.2 mA/cm^2 at 1.2 V *vs.* RHE	99.9% of 20 ppm 4-FP; 75.8 % of TOC (150 min)	11
WO_3/CdS/Co-Pi	0.1 M phosphate buffer solution + 0.5 M Na_2SO_3	5.85 mA/cm^2 at 1.23 V *vs.* RHE	H_2: - O_2: -	12
Mo:$BiVO_4$ nanoparticle-coated WO_3	0.5 M Na_2SO_4 + 0.1 M Na_2SO_3	5.8 mA/cm^2 at 1.23 V *vs.* RHE	H_2: - O_2: -	13
CoP/$BiVO_4$:WO_3	0.5 M Na_2SO_4	2.81 mA/cm^2 at 1.23 V *vs.* RHE	H_2: - O_2: -	14
WO_3/$BiVO_4$/NiOOH	2 M sodium borate (NaBi)	3.0 mA/cm^2 at 1.23 V *vs.* RHE	H_2: - O_2: -	15
WO_3/$BiVO_4$ core−shell hetero-nanostructure	0.5 M phosphate buffer (pH 7) with 1 M Na_2SO_3	4.15 mA/cm^2 at 1.23 V *vs.* RHE	H_2: - O_2: -	16
(WO_3/$BiVO_4$)-OV/CoPi	0.1 M Na2SO4 and 0.1 M KPi	2.3 mA/cm^2 at 1.23 V *vs.* RHE	H_2: - O_2: -	17
Cobalt–phosphate (Co–Pi) co-catalyst decorated WO_3/Mo-$BiVO_4$ photoanode	0.5 M K_2SO_4	5.38 mA/cm^2 at 1.23 V *vs.* RHE	H_2: - O_2: -	18
WO_3/$BiVO_4$-15	0.5 M Na_2SO_4	4.46 mA/cm^2 at 0.5 V *vs.* Ag/AgCl	H_2: 258.98 μmol/h/cm^2 99.34 % of 10 ppm RhB（60 min）	Our work

References

1 M. Tayebi, Z. Masoumi, M. Kolaei, A. Tayyebi, M. Tayebi, B. Seo, C.-S. Lim, H.-G. Kim and B.-K. Lee, *Chem. Eng. J.*, 2022, **446**, 136830.

2 F. Lin, Y.-Y. Gu, H. Li, S. Wang, X. Zhang, P. Dong, S. Li, Y. Wang, R. Fu, J. Zhang, C. Zhao and H. Sun, *Sci. Total Environ.*, 2021, **796**, 148931.

3 D. Coelho, J. P. R. S. Gaudêncio, S. A. Carminati, F. W. P. Ribeiro, A. F. Nogueira and L. H. Mascaro, *Chem. Eng. J.*, 2020, **399**, 125836.

4 R. Zhang, F. Ning, S. Xu, L. Zhou, M. Shao and M. Wei, *Electrochim. Acta*, 2018, **274**, 217-223.

5 K. Li, Y. Yin and P. Diao, *Small*, 2024, **20**, 2402474.

6 K.-H. Ye, Z. Wang, J. Gu, S. Xiao, Y. Yuan, Y. Zhu, Y. Zhang, W. Mai and S. Yang, *Energy Environ. Sci.*,

2017, **10**, 772-779.
7 X. Fan, Q. Chen, F. Zhu, T. Wang, B. Gao, L. Song and J. He, *Molecules*, 2024, **29**, 372.
8 B. Jin, E. Jung, M. Ma, S. Kim, K. Zhang, J. I. Kim, Y. Son and J. H. Park, *J. Mater. Chem. A*, 2018, **6**, 2585-2592.
9 Y. Li, Q. Mei, Z. Liu, X. Hu, Z. Zhou, J. Huang, B. Bai, H. Liu, F. Ding and Q. Wang, *Appl. Catal. B Environ. Energy*, 2022, **304**, 120995.
10 Q. Ma, R. Song, F. Ren, H. Wang, W. Gao, Z. Li and C. Li, *Appl. Catal. B Environ. Energy*, 2022, **309**, 121292.
11 Q. Ma, Z. Ning, M. Fang, G. Zhang, H. Guo, J. Zhou and T. Wang, *Chem. Eng. J.*, 2024, **498**, 155551.
12 J. Sun, L. Sun, X. Yang, S. Bai, R. Luo, D. Li and A. Chen, *Electrochim. Acta.* , 2020, **331**, 135282.
13 K. Kim, S. K. Nam, J. H. Park and J. H. Moon, *J. Mater. Chem. A*, 2019, **7**, 4480-4485.
14 N. D. Quang, P. C. Van, S. Majumder, J.-R. Jeong, D. Kim and C. Kim, *J. Alloys Compd.*, 2022, **899**, 163292.
15 W. Fang, Y. Lin, R. Xv and L. Fu, *ACS Appl. Energy Mater.*, 2022, **5**, 11402-11412.
16 B. R. Lee, M. G. Lee, H. Park, T. H. Lee, S. A. Lee, S. S. M. Bhat, C. Kim, S. Lee and H. W. Jang, *ACS Appl. Mater. Interfaces*, 2019, **11**, 20004-20012.
17 J. Liu, W. Chen, Q. Sun, Y. Zhang, X. Li, J. Wang, C. Wang, Y. Yu, L. Wang and X. Yu, *ACS Appl. Energy Mater.*, 2021, **4**, 2864-2872.
18 Q. Zeng, J. Li, L. Li, J. Bai, L. Xia and B. Zhou, *Appl. Catal. B Environ. Energy*, 2017, **217**, 21-29.